Unoccupied surface states on Cu(001): A comparison of experiment and theory

S. L. Hulbert, P. D. Johnson, and M. Weinert
Brookhaven National Laboratory, Upton, New York 11973

R. F. Garrett*
State University of New York at Stony Brook, Stony Brook, New York 11794
(Received 10 September 1985)

We compare new high-resolution inverse-photoemission spectra of the unoccupied surface states on Cu(001) with a first-principles calculation of the same surface. This theoretical calculation includes the asymtotic long-range image potential. The commonly observed image state is found to correspond to the $n=1$ member of the Rydberg series of states derived from the image potential, i.e., the wave function has a single extremum beyond the crystal edge characteristic of the hydrogenic $n=1$ state. Agreement between theory and experiment for all states is excellent. The experimentally determined binding energies and effective masses are 0.62 eV and $0.98m_e$ for the $n=1$ image state and 0.8 eV (with respect to E_F) and $0.4m_e$ for the $n=0$ surface resonance. The results indicate that surface corrugation effects are negligible.

I. INTRODUCTION

Recently there have been several inverse-photoemission studies of unoccupied surface states on metal surfaces.[1-10] These studies have tended to classify the states into two categories: those derived from the crystal potential termination at the vacuum interface and those derived from the long-range image potential experienced by an electron outside of the surface.

A simple one-dimensional multiple-reflection model was originally proposed to account for the binding energies of the image states.[11] The first demonstration that this model could be used to account for the variation in the binding energies of these states on different surfaces[10] produced the interesting result that the same model successfully accounted for the binding energies of the crystal-derived states on these surfaces. The binding energy of the image states was shown to be influenced by the position of the vacuum level with respect to the nearly-free-electron band gap generated by the appropriate reciprocal-lattice vector running perpendicular to the surface.

An alternative model has also been proposed[12] in which it was suggested that the binding energies of the image states and their effective masses were dominated by the surface corrugation running parallel to the surface. In this model second-order perturbation theory was used to show that interaction with the surface corrugation causes the simple hydrogenic series derived from the image potential to be pushed to significantly larger binding energies.

More recently we have been able to apply wave-function matching techniques to these problems and have demonstrated,[13] for the first time in a mathematically rigorous formalism, the connection between the image states and the crystal-derived states. We have further demonstrated the role of the image plane in defining the boundary condition which determines the binding energy of these states. Surface corrugation was found to play a role only in that the packing density of the surface determined the position of the image plane. In particular, the image plane was found to be further from the crystal edge, defined as half a lattice spacing beyond the last row of atoms, on more loosely packed surfaces. However, as the crystal edge is closer to the center of the last row of atoms on more loosely packed surfaces, it is probably more appropriate to define the image plane in terms of electron density calculated from the center of the last row of atoms. Defined in this way our analysis demonstrated that the image plane would be in a similar position for all low-index surfaces of a given metal.

In this paper we present new high-resolution experimental measurements of the binding energies and effective masses of unoccupied surface-derived features on the Cu(001) surface. We compare these observations with the results of a first-principles full-potential linearized augmented-plane-wave (FLAPW) calculation of the surface states on the same surface. In the calculation the image states are derived by matching a long-range image potential onto the self-consistent crystal potential. This calculation allows us to examine the effects of corrugation on the surface states, and we are able to discuss the relevance of the models previously proposed.

In Sec. II we present our experimental methods, and in Sec. III we discuss the theoretical procedures used. In Sec. IV we present the experimental results, and in Sec. V we compare these results and discuss them in terms of the theoretical results and the simple models.

II. EXPERIMENTAL METHODS

The experiments described here employ a new grating spectrograph which allows photons in the energy range from 10–30 eV to be detected. This instrument, which will be described in detail elsewhere,[14] employs the focused spot of the electron beam as a virtual entrance slit

and is capable of obtaining a wavelength resolution of the order of 10 Å. At 15 eV the energy resolution is therefore approximately 0.18 eV. The electron source has been described elsewhere[15] and provides currents of the order of 10 μA with an energy spread of 0.25 eV. The full angular spread of the incident beam is 5 ° corresponding to a momentum resolution $\Delta k_{||}$ of approximately 0.17 Å at 15 eV; the overall experimental resolution at this energy is 300 meV.

Measurements are made by fixing the incident electron energy and incidence angle, and then monitoring all direct transitions at different photon energies in parallel. With instruments of this type it is possible to monitor the dispersion of surface states either by rotating the sample at fixed incident energy or by fixing the incidence angle and then recording spectra for different incident energies.

The copper (001) crystal was cleaned by repeated cycles of argon bombardment and annealing, and the surface condition was monitored by Auger-electron spectroscopy and low-energy electron diffraction (LEED).

III. THEORETICAL METHODS AND RESULTS

The electronic structure of the ideal Cu(001) surface was calculated using the self-consistent FLAPW method.[16] This method has been shown to give very accurate solutions to the density-functional equations. The surface was modeled by using a slab of seven layers of copper. No shape approximations were made to either the density or potential, and all non-muffin-tin contributions to the Hamiltonian were taken into account self-consistently. The standard local-density approximation[17] (LDA) to the exchange-correlation potential was used in the self-consistency cycle. Once self-consistency was achieved, a final iteration was performed using a modified potential[18] that correctly includes the image form for large distances. This modification did not significantly affect the previously calculated ground-state density and position of the crystal-derived surface states and resonances, since little electron density extends into this asymptotic region in which the LDA breaks down. The image plane is located in a position such that the electron-gas parameter r_s of the planar average density is approximately 5.0.

The addition of the long-range image potential produced, as expected, a Rydberg-like series of unoccupied states bound close to the vacuum level. While both the crystal-derived and image-derived surface states can be understood within the same framework,[13] we have a simple calculational criterion for distinguishing between them: Those states which are found in the calculation only with the inclusion of the image potential are defined as image states; all others are called crystal derived. This same criterion may be arrived at using the phase model where the conventional or crystal-derived states can be modeled with a simple-step potential for the surface barrier.[9,19]

Crystal-derived unoccupied surface states around $\bar{X}$ exist at the top and bottom of the band gap, and a surface resonance at $\bar{\Gamma}$ exists below the bottom of the gap. The calculated energy of the high-lying surface state at $\bar{X}$ is $\approx$0.2 eV below the top of the gap with an effective mass of $m^* \approx 1.8 m_e$. At the bottom of this gap we find an occupied state 0.07 eV below the Fermi level with effective mass $m^* \approx 0.06 m_e$. The surface resonance at $\bar{\Gamma}$ is calculated to lie 0.5 eV above the Fermi level and corresponds to the "$n=0$" state of Hulbert *et al.*[10,13] This state is not as localized to the surface region as are the states at $\bar{X}$ and the occupied d-derived surface states. For this reason, this state (and its counterparts on other surfaces) has not been identified as a resonance in other calculations. The existence of these surface states and resonances can be obtained from general resonance scattering arguments.[13] The calculated effective mass of this state at $\bar{\Gamma}$ is $m^*=0.49$ near the center of the zone; if one calculates m^* using points halfway to the zone boundary, this value increases to $m^*/m_e \approx 0.7$ since the dispersion of the band is nonparabolic.

As already stated, the inclusion of the image potential in the calculations gives an additional set of states near the vacuum level that do not exist in the LDA calculation. These we identify as the image states. We label the "principal quantum number" in terms of the number of extrema of the wave functions of these states beyond the crystal edge and, in analogy with quantum defect theory in atoms, in terms of the binding energy. While other labeling choices are of course possible, we believe ours is the most reasonable physically and is consistent with standard usage in other fields.[13] The first three members ($n=1,2,3$) of the series have binding energies of 0.62, 0.19, and 0.09 eV, respectively. These states all have $m^*/m \approx 1$. Corrugation of the classical image potential and the Coulomb potential has no appreciable effect on the effective mass since these corrugations decay exponentially, i.e., the corrugation matrix element for an image state whose weight is several angstroms outside the surface is negligible. As discussed elsewhere,[13] dynamical contributions to the image potential not included here lead to an increase in the effective mass by $<5\%$.

IV. EXPERIMENTAL RESULTS

In Fig. 1 we show inverse photoemission spectra for different angles of incidence in the $\bar{\Gamma}\bar{M}$ azimuth near the center of the zone. The electron beam is incident on the surface with an energy of 16.85 eV with respect to the Fermi level. We identify the sharp feature, which has a binding energy (defined with respect to the vacuum level) of approximately 0.6 eV at the center of the zone, with the first member of the Rydberg series of image states.

At this initial energy there are no allowed bulk transitions. We are therefore able to make the more definite assignment of surface resonance to the feature just above the Fermi level. This resonance was predicted earlier by the multiple-reflection model,[10] and appears in the first-principles calculation as described in the preceding section. Its observation has been noted in previous work,[8] but the tunability of photon detection and the improved resolution allow this state to be clearly resolved from any bulk-derived features in the present work.

Using a least-squares-fitting procedure, we find that the image state has an effective mass of $0.98 \pm 0.10 m_e$ and a

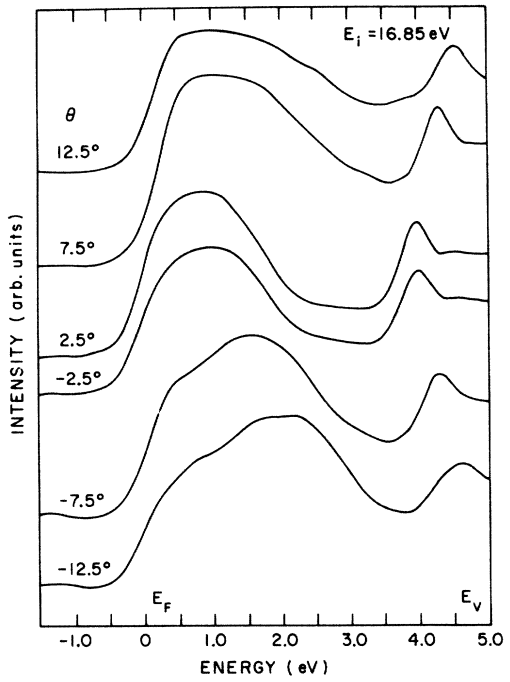

FIG. 1. Inverse photoemission spectra recorded for the Cu(001) surface as a function of the angle of incidence in the $\bar{\Gamma}\bar{M}$ azimuth. The initial energy of the electron beam was 16.85 eV with respect to the Fermi level.

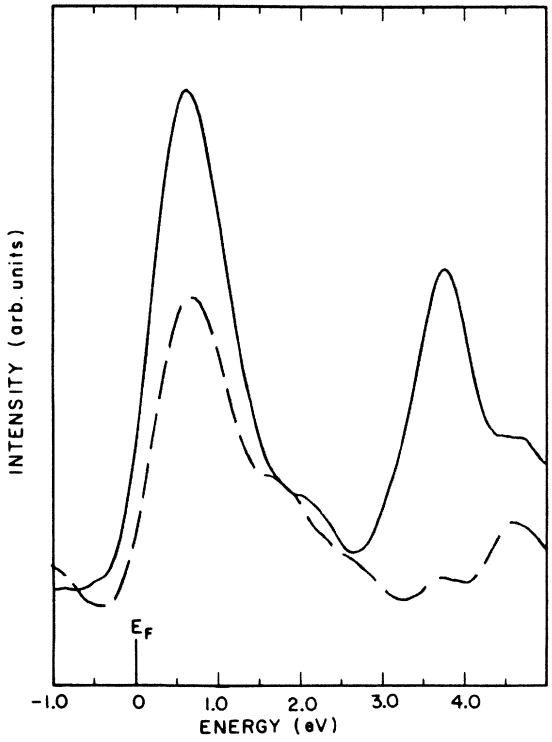

FIG. 2. Inverse photoemission spectra recorded at the $\bar{X}$ point of the surface Brillouin zone of Cu(001) with initial electron energy 16.5 eV above the Fermi level. Clean surface (solid line) and same surface after exposure to 40 L of oxygen (dashed line).

binding energy at the center of the zone of 0.62 ± 0.05 eV. The surface resonance, however, is not an easy feature to locate exactly; the experiments would indicate that near the center of the zone the effective mass is approximately $0.4m_e$ at an energy approximately 0.8 eV above the Fermi level. Fitting more distant points in the zone, the effective mass increases to $0.6m_e$ for measurements out to $0.25\bar{\Gamma}\bar{M}$.

At $\bar{X}$ we identify two features as shown in Fig. 2. This figure also shows the effect of exposing the surface to 40 L of oxygen. [1 langmuir (L)$\equiv 10^{-6}$ Torr sec.] We associate the peak close to the Fermi level in Fig. 2 with a mixture of the low-lying surface state and, due to our more limited momentum resolution at high angles of incidence, transitions into bulk band 6. We are clearly able to identify the peak at lower binding energy as the surface state predicted to lie near the top of the gap. Our studies of this state have tended to concentrate on its cross-sectional behavior,[20] and we have thus not made any detailed studies of its dispersion. However, our limited studies around $\bar{X}$ indicate a relatively high effective mass for this state.

V. DISCUSSION

Both the experimental observations and the theoretical calculations contain a peak approximately 0.62 eV below the vacuum level with a free-electron-like dispersion. This state, which we identify with the $n=1$ member of the Rydberg series of image states, has been observed in a number of earlier studies of Cu(100),[1,4,5] and a similar feature has also been observed on Ag(100).[12] We note, however, that the effective mass that we measure in this study is lower than previous measurements on either Cu(100) (Ref. 5) or Ag(100) (Ref. 12). The present study represents the first study with good energy resolution combined with reasonable momentum resolution. We therefore feel confident in making comparisons with our first-principles theory.

In the study of Ag(100),[12] it was suggested that the peak at 0.6-eV binding energy was, in fact, the $n=2$ member of the Rydberg series shifted to higher binding energy through the perturbative effect of surface corrugation. The present study disagrees with that conclusion and suggests that the wave function for this state has the characteristic shape of an $n=1$, rather than an $n=2$, hydrogenic wave function. In Fig. 3 we show the charge densities of the first three members of the Rydberg series of states as produced in the FLAPW calculation.

We note that the FLAPW calculation and our wave-function matching technique[13] produce nearly identical wave functions for the image states. We also note that the maximum for the $n=1$ wave function on this surface is displaced further from the crystal edge than for the same state on the Cu(111) surface, 3.5 rather than 2.0 Å. On the Cu(001) surface this image state is closer to the center of the band gap than on the Cu(111) surface; near the center of such a gap, the penetration into the crystal will be less (the decay length is less), and as a result one would expect the image state to be pushed further into the vacuum.

We note again that both the measured effective mass of

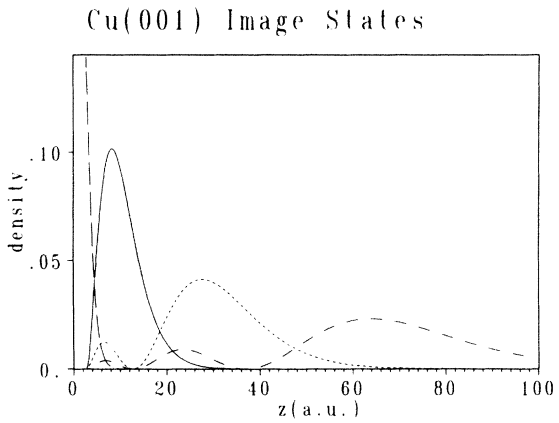

FIG. 3. Charge densities of the Rydberg series of image states and surface resonance averaged parallel to the surface. Image states: $n=1$ (solid line) (0.62 eV), $n=2$ (short-dashed line) (0.19 eV), and $n=3$ (long-dashed line) (0.09 eV); surface resonance (dashed-dotted line). Zero on the distance scale corresponds to the center of the last row of atoms.

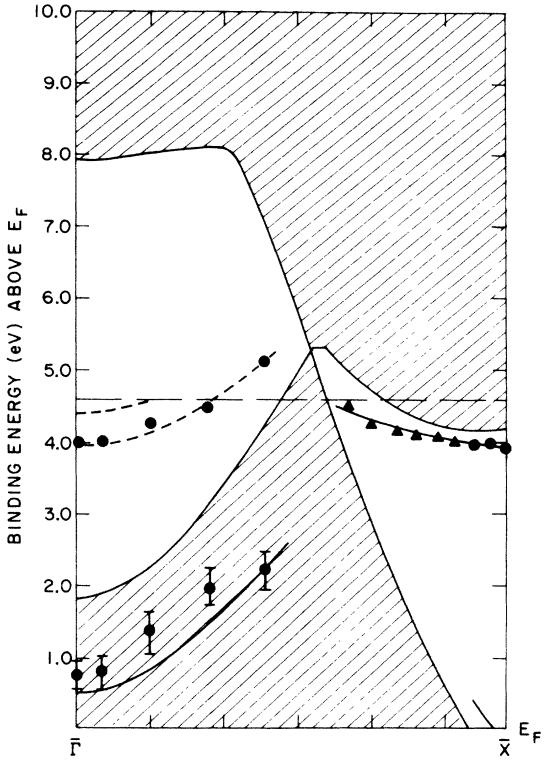

FIG. 4. Comparison of theoretical and experimental results. The crosshatched area represents the projected bulk continuum; solid lines (dashed lines) represent the theoretical predictions of the crystal-potential-derived (image-potential-derived) surface states. ●, experimental results from the present study. ▲, experimental results from Ref. 5.

this state and the calculated mass are close to $1.0m_e$. Furthermore, in our calculation it is possible to "switch-off" the surface corrugation outside of the jellium or crystal edge. We find that this produces *no appreciable effect* on either the binding energy or the effective masses of the Rydberg series of image states.

The surface resonance at $\bar{\Gamma}$ has a smaller effective mass than the observed image state, being approximately $0.4m_e$ near the center of the zone and increasing to approximately $0.6m_e$ as one proceeds further out in the zone. Previously, we published the energy of this state as 1.15 eV above the Fermi level.[8] That value was produced from Lorentzian fitting to data of lower resolution. Here we find an experimental value of 0.8 eV above the Fermi level. However, we note that we are attempting to identify the center of an extremely broad feature, characteristic of a surface resonance. We would therefore probably have to conclude that this resonance is of the order of 1.0 eV above the Fermi level, but erring towards the binding energy measured in the present experiment. The FLAPW calculation produces an energy of 0.5 eV with respect to the Fermi level. The exact position of this calculated resonance is rather uncertain due to the finite thickness of the film. For finite films, one does not obtain a continuum of states corresponding to the projection of the bulk bands, but rather a set of discrete $2-d$ bands whose energy separation is indicative of the number of layers and the width of the bulk bands perpendicular to the surface. The calculated position of the resonance is then given by the energy of the discrete band closest to the true energy. In contrast, a surface state split off into a bulk band gap does not couple to the bulk Bloch waves running perpendicular to the surface and hence can, in general, be described by a combination of orbitals localized near the surface. True surface states are therefore treated "correctly" in a thin-film method, and the uncertainty in the calculated energies is significantly smaller than for resonances.

The phase model produces an energy of 1.2 eV above the Fermi level for the surface resonance.[8,10] This value may well be too high because the model assumes that r_c, the reflectivity from the crystal, has the value of 1.0. This will be true for band gaps but not in the continuum region. We further note that the phase model[10,19] places the image plane at the crystal edge. Our more recent wave-function matching technique[13] places the image plane beyond the crystal edge, producing a surface resonance at 0.9 eV above the Fermi level.

We are unable in the present study to learn anything new about the low-lying surface state at $\bar{X}$. However, we note good agreement between the theoretical results presented here and the earlier studies of Kevan,[21] the binding energy of the state being approximately 0.07 eV below the Fermi level and the effective mass being $0.06m_e$.

We find the higher surface state at $\bar{X}$ to have an energy of approximately 3.9 eV above the Fermi level. As stated earlier, we were unable to measure the effective mass of this state in the present study. However, our data combined with the earlier date of Dose *et al.* (Fig. 4) shows that the effective mass of this state is in close agreement with the theoretical value presented in this paper.

In summary, we have compared experimental and theoretical binding energies, and in some cases effective masses, for all unoccupied surface states on Cu(001). The

calculated and measured dispersions of all of these states are compiled in Fig. 4. The cross-hatched area represents the continuum of bulk states and is calculated using the 16 plane-wave version of the combined interpolation scheme.[22] The parameters used for Cu(001) were taken from Ref. 22 and optimized to fit the empty bands.[20] It can be seen that reasonable agreement is obtained between theory and experiment for all states.[23] From a calculational view these states, although related, fall naturally into two classes: those derived from the crystal termination and those derived from the long-range image potential. We find that the image states at the center of the zone are unaffected by surface corrugation and that the image state observed experimentally is the state whose wave function has a single maximum ≈ 3.5 Å beyond the crystal edge.

We acknowledge useful discussions and advice from N. V. Smith. This work was supported by the Division of Materials Science, U.S. Department of Energy under Contracts No. DE-AC02-76CH00016 and No. DE-AC02-80ER10750.

---

*Present address: National Synchrotron Light Source, Brookhaven National Laboratory, Upton, NY 11973.

[1]P. D. Johnson and N. V. Smith, Phys. Rev. B **72**, 2527 (1983).
[2]B. Reihl, R. R. Schlittler, and H. Neff, Phys. Rev. Lett. **52**, 1826 (1984).
[3]V. Dose, W. Altmann, A. Goldmann, V. Kolac, and J. Rogozik, Phys. Rev. Lett. **52**, 1919 (1984).
[4]D. Straub and F. J. Himpsel, Phys. Rev. Lett. **52**, 1922 (1984).
[5]V. Dose, V. Kolac, G. Borstel, and G. Thörner, Phys. Rev. B **29**, 7030 (1984).
[6]D. A. Wesner, P. D. Johnson, and N. V. Smith, Phys. Rev. B **30**, 503 (1984).
[7]B. Reihl, K. H. Frank, and R. R. Schlittler, Phys. Rev. B **30**, 7328 (1984).
[8]D. P. Woodruff, S. L. Hulbert, P. D. Johnson, and N. V. Smith, Phys. Rev. B **31**, 4046 (1985).
[9]R. A. Bartynski, T. Gustafsson, and P. Soven, Phys. Rev. B **31**, 4745 (1985).
[10]S. L. Hulbert, P. D. Johnson, N. G. Stoffel, W. A. Royer, and N. V. Smith, Phys. Rev. B **31**, 6815 (1985).
[11]P. M. Echenique and J. B. Pendry, J. Phys. C **11**, 2065 (1978).
[12]N. Garcia, B. Reihl, K. H. Frank, and A. R. Williams, Phys. Rev. Lett. **54**, 591 (1985).
[13]M. Weinert, S. L. Hulbert, and P. D. Johnson, Phys. Rev. Lett. **55**, 2055 (1985).
[14]P. D. Johnson, S. L. Hulbert, R. F. Garrett, and M. R. Howells (unpublished).
[15]N. G. Stoffel and P. D. Johnson, Nucl. Instrum. Methods A **234**, 230 (1985).
[16]E. Wimmer, H. Krakauer, M. Weinert, and A. J. Freeman, Phys. Rev. B **24**, 864 (1981); M. Weinert, J. Math. Phys. **22**, 2433 (1981).
[17]W. Kohn and L. J. Sham, Phys. Rev. **140**, A1133 (1965); L. Hedin and B. I. Lundquist, J. Phys. C **4**, 2064 (1971).
[18]M. Weinert, Bull. Am. Phys. Soc. **30**, 409 (1985); and unpublished.
[19]N. V. Smith, Phys. Rev. B **32**, 3549 (1985).
[20]S. L. Hulbert, P. D. Johnson, and R. F. Garrett (unpublished).
[21]S. D. Kevan, Phys. Rev. B **28**, 2268 (1983).
[22]N. V. Smith, Phys. Rev. B **19**, 5019 (1979).
[23]We note that in Fig. 4 the experimental results relating to the states around the center of the zone were actually recorded in the $\bar{\Gamma}\,\bar{M}$ azimuth rather than the $\bar{\Gamma}\,\bar{X}$ azimuth. Our limited experimental data shows that this is not unreasonable as the states are azimuthally symmetric near the center of the zone; this is also in agreement with the theoretical calculation.